Title

Diffusion Tensor Imaging-Based Thalamic Segmentation in Deep Brain Stimulation for Chronic Pain Conditions

Journal

Stereotactic and Functional Neurosurgery, 94(4)

ISSN

1011-6125

Authors

Kim, Won
Chivukula, Srinivas
Hauptman, Jason
et al.

Publication Date

2016

DOI

10.1159/000448079

Peer reviewed

Published in final edited form as:

Stereotact Funct Neurosurg. 2016 ; 94(4): 225–234. doi:10.1159/000448079.

Diffusion Tensor Imaging Based Thalamic Segmentation in Deep Brain Stimulation for Chronic Pain Conditions

Won Kim, M.D.[a], **Srinivas Chivukula, M.D.**[a], **Jason Hauptman, M.D., Ph.D.**[a], and **Nader Pouratian, M.D., Ph.D.**[a,b,c,d]

[a]Department of Neurological Surgery, University of California, Los Angeles, 10945 Le Conte Ave Suite 2120, Los Angeles, CA 90095

[b]Interdepartmental Program in Neuroscience, University of California, Los Angeles, 10945 Le Conte Ave Suite 2120, Los Angeles, CA 90095

[c]Department of Bioengineering, University of California, Los Angeles, 10945 Le Conte Ave Suite 2120, Los Angeles, CA 90095

[d]Brain Research Institute, University of California, Los Angeles, 10945 Le Conte Ave Suite 2120, Los Angeles, CA 90095

Abstract

Background/Aims—Thalamic deep brain stimulation (DBS) for the treatment of medically refractory pain has largely been abandoned on account of its inconsistent and oftentimes poor efficacy. Our aim here was to use diffusion tensor imaging (DTI)-based segmentation to assess the internal thalamic nuclei of patients who have undergone thalamic DBS for intractable pain and retrospectively correlate lead position with clinical outcome.

Methods—DTI-based segmentation was performed on 5 patients who underwent sensory thalamus DBS for chronic pain. Postoperative computed tomography (CT) images obtained for electrode placement were fused with preoperative MRIs that had undergone DTI-based thalamic segmentation. Sensory thalamus maps of 4 patients were analyzed for lead positioning and interpatient variability.

Results—Four patients who experienced significant pain relief following DBS demonstrated contact positions within the DTI-determined sensory thalamus or in its vicinity, whereas one who did not respond to stimulation did not. Only four voxels (2%) within the sensory thalamus were mutually shared among patients; 108 voxels (58%) were uniquely represented.

Conclusions—DTI-based segmentation of the thalamus can be used to confirm thalamic lead placement relative to the sensory thalamus, and may serve as a useful tool to guide thalamic DBS electrode implantation in the future.

Corresponding Author: Won Kim, M.D. Department of Neurological Surgery, UCLA Health System, 11822 Kiowa Ave Apt 10, Los Angeles, CA 90049, wonkim@mednet.ucla.edu.

Conflicts of interest

The authors have no financial or other relationships to disclose that may be a potential conflict of interest to the research being presented.

Financial Disclosure/Disclaimer: The authors have no vested financial interests in this study.

Keywords

DBS; Deep brain stimulation; DTI; Diffusion Tensor Imaging; Pain; Thalamic segmentation

INTRODUCTION

Electrical stimulation of deep brain structures to treat both nociceptive and neuropathic varieties of chronic pain syndromes has been in practice for over half a century [1,2]. Yet recent meta-analyses indicate that only approximately 60% of patients with nociceptive pain syndromes, and 40% of those with neuropathic pain, benefit from deep brain stimulation (DBS). Notably, their preferred central neuromodulatory targets differ; whereas the periaqueductal (or periventricular) grey (PAG/PVG) is the target of choice for nociceptive pain, the ventroposteromedial (VPM) and ventroposterolateral (VPL) thalamus (sensory thalamus) are preferred for neuropathic pain [2,3].

Reasons for the heterogeneity in patient responsiveness to DBS for chronic pain syndromes remain elusive, but it is consensually accepted that targeting is critical to successful neuromodulation [4,5]. The “sensory” thalamus is currently targeted for DBS implantation indirectly, using stereotactic atlases and relying on intraoperative patient feedback in response to acute stimulation to guide final electrode positioning. Standard magnetic resonance imaging (MRI) and computed tomography (CT) scans do not provide adequate thalamic internal anatomic detail, possibly leading to inappropriate targeting and subsequently, to poor clinical response. Ideally, targeting should be based on patient-specific anatomic information.

Diffusion tensor imaging (DTI) has demonstrated utility in patient-specific thalamic anatomical targeting in numerous studies of DBS implantation for tremor [6–10]. As a case in point, our group recently reported anatomically segmenting the thalamus using DTI and probabilistic tractography to define the optimal area for targeting within the thalamus for tremor control by neuromodulation; it was our observation that thalamic nuclei demonstrate internal consistency but vary considerably from subject to subject and from subject to atlas, suggesting that the location of thalamic DBS targets for pain may also be similarly variable [9]. Although they may be identifiable reliably, we hypothesized that the targets may demonstrate atlas-subject and/or intersubject variability.

We herein present retrospective analyses of five patients who underwent DBS for chronic pain syndromes at our institution, with a view to better define the role of DTI based thalamic segmentation in guiding thalamic DBS for pain. We conjectured that the use of DTI based probabilistic tractography could not only identify the VPL/VPM, but also determine whether the implanted electrodes are in a position to effectively stimulate these target nuclei and provide adequate pain relief. The goal was to gain insight into whether poor clinical responses are failures of optimally targeted stimulation or at least in part, sequelae of inappropriate targeting.

METHODS

Study population

Following institutional review board approval at our institution, seven patients were identified who underwent deep brain stimulation of the sensory thalamus (VPL/VPM), with or without an additional lead in the periaqueductal grey. Five (two male, three female) of these seven patients had the appropriate imaging and clinical follow-up and were included in our analyses. Their demographics are shown in Table 1. Their mean age was 56 ± 14.8 years (range 46–81). Indications for DBS included Dejerine-Roussy syndrome, brachial plexus avulsion (BPA), spinal cord injury (SCI; traumatic L1 fracture) with resultant paraplegia and neuropathic pain, postherpetic neuralgia (PHN), and complex regional pain syndrome type I (CRPS I) or reflex sympathetic dystrophy (RSD) secondary to brachial plexus injury. All patients were previously evaluated, medically managed, and referred by pain management specialists.

Other neuromodulatory therapies prior to DBS included motor cortex stimulation (MCS), cranial epidural stimulation, DBS itself (five years earlier, at another institution), and intrathecal pain pump placement and spinal cord stimulation (SCS). One patient underwent placement of an epidural spinal cord stimulator between reprogramming sessions on account of the inadequate pain control from DBS and medications.

Surgical procedure

Four of the five patients underwent high resolution 3T MR imaging within the week prior to surgery. On the day of surgery, a Leksell frame was placed using local anesthesia, and an intraoperative CereTom (http://www.neurologica.com/ceretom.html) CT was obtained. The preoperative MRI images were subsequently fused to these intraoperative images for surgical planning using BrainLab software. One patient underwent preoperative MR imaging in the 1.5T intraoperative MRI, which was used for target localization and trajectory planning. The VPL/VPM thalamus in all patients was targeted based on coordinates obtained from the Schaltenbrand-Wahren Atlas. Specifically, we targeted a region approximately 10–12 mm lateral from the third ventricular wall (depending on area of pain) and 10–12 mm posterior to the midcommissural point (MCP).

For stereotactic implantation, the Leksell frame was fixed to the operating room table with the patient positioned in a semi-reclined position with head flexed slightly. A radiofrequency electrode was advanced in a sterile fashion to target after dural opening. The DBS lead (Medtronic 3387, Medtronic Inc., Minneapolis MN, USA) was then inserted to the planned depth, and stimulation performed to assess for sensory sequelae. When it was felt that adequate paresthesias were induced from stimulation, the lead was secured in place. Leads were repositioned intraoperatively according to patient response to stimulation (Patients 1, 4 and 5) when the induced paresthesias were inadequate or unsatisfactory. Postoperative imaging (3 CT, 1 MRI) was obtained prior to leaving the OR to ensure adequate lead position. Generators were implanted in each case as a separate surgery approximately 2 weeks later.

Imaging analysis

Our methods for defining target and seed masks for probabilistic connectivity based tractography and thalamic segmentation have been described previously [9]. Similar to our earlier report, we delineated one seed mask (thalamus) and seven cortical target masks for each patient: prefrontal cortex, premotor cortex, primary motor cortex (M1), primary somatosensory cortex, temporal cortex, posterior parietal cortex, and occipital cortex. Their anatomical limits have been previously defined (http://www.fmrib.ox.ac.uk/connect/definitions.html). Cortical regions of interest (i.e. target masks for probabilistic tractography) were defined in an automated manner using LONI (Laboratory of Neuroimaging, University of California, Los Angeles) Brain Parser [11]. For the purposes of this study, the target masks from the postcentral gyrus (i.e., somatosensory cortices) bilaterally were the ones of interest in defining the sensory thalamus, although all were analyzed. The thalamus for each individual was likewise generated in an automated manner using FreeSurfer (http://surfer.nmr.mgh.harvard.edu/).

All analyses were run in an automated blinded manner, and probabilistic diffusion tractography was conducted using the LONI Pipeline platform and FSL tools (http://www.fmrib.ox.ac.uk/fsl) [12]. Specifically, the FMRIB's Diffusion Toolbox (FDT) was used to carry out the DTI-connectivity analysis. This toolset uses Bayesian techniques to estimate the probability function of principal fiber direction at each voxel. These probability distribution functions were then used to determine the likelihood of connectivity between the thalamic seed voxels and cortical targets. DTI data were unwarped and skull stripped using FDT's eddy current correction tool and FSL's brain extraction tool (BET), respectively. BEDPOSTX, a model that accounts for the possibility of crossing fibers within each voxel, was then used to calculate estimates of voxel-wise fiber orientations. The diffusion data were linearly registered (FLIRT) to the high resolution T1 weighted image and subsequently, PROBTRACKX (using 5000 samples, a 0.2 curvature threshold, and loop-check termination) was used to determine the probability of connectivity of each thalamic voxel with the sensory cortex based on the BEDPOSTX output, the transformation matrices, and the previously defined seed and target masks.

Connectivity-based segmentation revealed distinct thalamic regions with high connectivity with distinct cortical regions. The thalamic map of relative connectivity with somatosensory cortices (i.e., VPM/VPL) and the postoperative CT or MRI demonstrating final electrode positions were then aligned with preoperative imaging (FLIRT) to compare thalamic maps with lead and contact positions. To compare the relative position of the sensory thalamus as defined by probabilistic tractography across subjects we performed subsequent intersubject analyses and comparisons. Maps of the sensory thalamus for each patient as determined by probabilistic tractography were transformed into standard space (MNI-152) using both FLIRT (12 parameter) and FMRIB's non-linear image registration tool (FNIRT). The sensory thalami were then thresholded and binarized at 1500 using fslmaths to isolate areas of highest probability of containing sensory thalamus within each subject. The binarized thalami were then summed in common space to visually demonstrate the distribution of overlapping voxels of sensory thalamus between subjects in common space.

Radiographic localization of DBS contacts

In order to assess the proximity of each individual DBS contact with the tractography-determined sensory thalamus, we calculated the position of each contact in three-dimensional space. The four contacts on the Medtronic 3387 DBS lead are centered 2.25mm, 5.25mm, 8.25mm and 11.25mm from the tip of the lead. To determine these contact positions in three dimensional space, we identified the coordinates corresponding to the lead tip (x_t, y_t, z_t) and another point (a: x_a, y_a, z_a) along the length of the electrode distant from the approximate vicinity of the contacts. Assuming a linear trajectory of the DBS lead, the ratio of the distance from the lead tip to the center of each contact (c) relative to the distance from the tip to point "a" (d) should equal the ratio of this distance traversed in each independent vector component. Thus, for a point that is a distance "c" from the tip of the electrode,

$$c/d=(x_c-x_t)/(x_a-x_t)=(y_c-y_t)/(y_a-y_t)=(z_c-z_t)/(z_a-z_t)$$

which can be used to derive the (x_c, y_c, z_c) for each contact.

Data collection and statistical analyses

Follow-up was obtained via telephone interview questionnaires, as well as medical chart and imaging review. Information pertaining to the patients' pain, location, severity, treatment history, pain reduction and post-DBS treatment were extracted. A 10-point numerical rating scale (similar to the Visual Analog Scale) was used to record pain severity. Postoperative pain relief was determined at the time of maximal pain relief, as well as at the last follow-up available in all instance possible. Pain reduction was computed as the difference between preoperative pain score and postoperative pain score at the two different time points. Patient demographics, surgical characteristics and outcomes were analyzed using descriptive statistics. Data were collected using Microsoft Excel 2013 (Microsoft Corp, Seattle, WA, USA).

RESULTS

Clinical outcomes

Data pertaining to DBS targeting and outcomes are presented in Table 2. Five patients underwent placement of eleven DBS leads (5 PVG, 6 VPL/VPM). Four patients received unilateral VPL/VPM and PVG (two left, two right), whereas one patient received bilateral DBS leads to the sensory thalamus in addition to a PVG lead. There were no intraoperative complications or postoperative neurologic sequelae. Of note, DBS electrodes were repositioned for inadequate or unsatisfactory stimulation induced paresthesias in Patients 1, 4 and 5. All patients experiences paresthesias in the distribution of their pain with final electrode positioning. Patients were followed for a mean of 28.8 months (range, 2–48 months). Patient specific outcomes were as follows: Patient 1 experienced complete relief in his stabbing type pain, and significant relief in his burning type pain, reporting an overall reduction from a 9 to a 3 on the pain rating scale. Patient 2 experienced some short-term benefits, stating that his pain decreased from a 6 to a 2 (on the numerical rating scale) upon

initial programming. However, it regressed to and never improved beyond a 5 on subsequent programming sessions. This patient consequently received a spinal cord stimulator to augment his DBS and was subsequently lost to follow-up. Patients 3 and 5 experienced moderate to significant pain relief with DBS at their latest follow-up post implantation. Patient 4 did not experience any initial benefit from DBS, however once the thalamic stimulator was turned off (1 year postoperatively) he had good pain control for one year with PVG stimulation alone. Patients 3 and 5 were still experiencing adequate pain control at their last follow-up (2 and 14 months, respectively).

Radiographic assessment of sensory thalamus and contact position

Non-responder—Patient 2's leads were found to be medial to the regions with the highest probability of containing VPL/VPM fibers/nuclei (Figure 1).

Responders—Localization of individual contacts per the aforementioned methods revealed that the patients with the best clinical response (Patients 3, 4 and 5) had DBS contacts within the region of thalamus with the highest probability of connectivity with the somatosensory cortex. Patient 1 experienced complete relief in his stabbing pain but only partial relief in his burning pain; this may relate to the fact that although contact 3 was appropriately positioned within the sensory thalamus, contacts 0, 1 and 2 were outside of the diffusion imaging based depiction of the sensory thalamus (Figure 2). Patient 3 had the best clinical response to contacts 1 and 2, which were the most appropriately located within the VPM/VPL map delineated by diffusion based tractography (Figure 3). Similarly, in Patient 4, contacts 0, 1, and 2 were located near the sensory thalamus, and he received the most benefit from contacts 1 and 2. In Patient 5 too, DTI-based segmentation of the thalamus revealed that the final electrode position was within the sensory thalamus and this patient received good benefit, most significantly from contacts 1,2, and 3, and likely with contribution from contact 1 as well (Figure 4).

Intersubject variability in sensory thalamus representation—Of the five patient scans, one could not undergo non-linear transformation given the degree of contrast enhancement within the scan affecting the transformation within FSL. The sum of the four binarized sensory thalamus maps visually demonstrated the distribution of VPL/VPM voxels commonly represented by subjects in MNI space (Figure 5). There were only 4 voxels that contained sensory thalamus representation from all 4 patients (2%). With these four voxels, there were also 36 voxels that represented sensory thalamus from 3 out of 4 patients, and these two groups comprised a central core region with highest commonality between subjects (yellow voxels). In the periphery, there were 38 voxels that represented VPL/VPM thalamus from 2 patients and 108 voxels (58%) that denoted unique patient representations of sensory thalamus.

DISCUSSION

Significant research has been dedicated to DBS for chronic pain [3,13–20]. A meta-analysis in 2005 by Bittar and colleagues revealed that stimulation of the PAG and VPL/VPM yielded greater long-term pain alleviation (87%) than stimulation of either the PAG alone

(79%) or the VPL/VPM alone (58%); moreover, thalamic DBS yielded relief in a greater fraction of patients with nociceptive pain (63%) than in those with neuropathic pain (47%) [3]. These findings were echoed more recently by Levy et al., who noted a greater rate of long-term pain control following thalamic DBS in patients with nociceptive pain (61%) when compared to that in those with neuropathic pain (42%); optimal targets for deep brain neuromodulation appeared to be the PAG for those with nociceptive pain, and the sensory thalamus for those with neuropathic pain, possibly with stimulation of both areas in all instances [2].

Failures may at least in part be attributable to an inability to optimally target the VPL/VPM nuclei. The lack of a discernible internal thalamic architecture in imaging modalities traditionally used for DBS limits the utility of standard image guidance in refining the targeting of the sensory thalamus. We therefore sought to evaluate a method for targeting the sensory thalamus utilizing connectivity based internal thalamic segmentation, by retrospectively analyzing the clinical outcomes of five patients implanted with DBS electrodes in the sensory thalamus for chronic pain in relation to the position of the electrodes on DTI based thalamic maps. The results of our analyses indicate that (1) DTI maps correlate with low threshold paresthesias, and (2) patients in whom the DBS electrodes were within the DTI target fared better than those in whom the electrode (or specific contacts) was not.

Stereotactic methods currently rely on indirect localization through the use of brain atlases derived from single subjects, with subsequent adjustments based on preoperative image guided planning and intraoperative neurophysiological assessment. Although neurophysiological testing may help guide the repositioning of leads, the need for repeated passes to elicit the clinical response presumed to result in favorable outcomes (e.g. paresthesias) increases the operative time as well as the risk of hemorrhage. The use of novel imaging techniques to delineate the internal structure of the thalamus to potentially guide stereotactic placement of leads for targets such as the ViM for essential tremor has been previously reported [26,30]. However, these methods focus on improving image acquisition to enhance structural contrasts rather than on elucidating functional connectivity or evaluating the efficacy of DBS.

In contrast, we previously demonstrated reliably delineating the internal nuclear structure of the thalamus utilizing probabilistic connectivity based segmentation [9]. Herein, we present an application of these methods to retrospectively analyze the targeting of the VPL/VPM thalamic sensory nuclei in DBS for chronic pain conditions in five patients. To our knowledge, this represents the largest such series, and only the second to date [16]. Our results demonstrate that those patients with the most overlap between electrode position and areas with the highest probability of containing VPL/VPM fibers (light blue) had superior pain relief with stimulation (Patients 1,3,4 and 5). Additionally, through an assessment of individual contact positions with our segmentation maps, we could retrospectively confirm that the contacts (leads) with the greatest overlap with the sensory thalamus provided the greatest clinical benefit to these patients.

Studies in non-human primates have shown that the thalamic ventrobasal complex (the caudal division of the VPL nucleus and the large-celled portion of the ventroposteromedial nucleus) project to primary and secondary somatosensory areas (S1 and S2) [23–31]. In humans, the ventroposterior nuclei (VPL and VPM) have the strongest probability of primary somatosensory cortical connectivity. We have found in our series that slight differences exist in the images regarding the localization and shape of the VPL/VPM nuclear complex between subjects and even nuclei in the same subject. In part, this would explain some results in our series. Electrodes in Patients 3,4 and 5 in our series were all eventually within the target determined by DTI based segmentation of the thalamus. Yet, the electrodes had to be repositioned in Patients 4 and 5, in one patient medially and in another patient posteriorly, relative to their initial placement based on standardized atlas based representations of the ventral posterior nuclear group, the sensory thalamus.

Although there is a small region in which the majority of subjects demonstrate overlap in the localization of VPL/VPM fibers, there is a great degree of variability within the immediate periphery (Figure 5). The majority (108 voxels or 58%) of sensory thalamus representation exhibited patient uniqueness. Notably, this variability exists despite non-linear transformation to a common space (MNI152), which accounts for differences in ventricular size, cerebral atrophy, and gross intracranial volume, without which would likely result in even greater apparent differences between patients. Additionally, thalamocortical fibers carrying information regarding pain probably exhibit patient specific spatial organization within the sensory thalamus. A case in point here is Patient 1, in whom stabbing type pain completely resolved at last follow up, but burning type pain persisted partially; this may be from a combination of two main factors, namely a single contact only being in the vicinity of the sensory thalamus, and/or the generated pulse frequency stimulation within the sensory thalamus not being sufficient.

This accentuates the importance of targeting based on individual functional anatomy. Moreover, as the putative mechanism through which patient’s achieve pain relief is through the modulation of thalamocortical networks, it is crucial to identify and target the regions that are functionally significant, rather than target those with radiographic or histologic significance. The reliable placement of leads in the VPL/VPM nuclei based on individualized thalamic anatomy could allow for implantation without clinical neurophysiological assessment or microelectrode recordings, shortening operative times and eliminating patient discomfort associated with wakefulness during the procedure. Furthermore, directly visualizing the DTI-determined sensory thalamus to guide initial targeting may minimize electrode passes, reducing the risk of hemorrhage [32,33]. Finally, by evaluating each electrode in relation to its vicinity to the sensory thalamic fibers, one can potentially use these patient-specific maps to guide programming and patient management.

Limitations

It is important to understand key limitations of our study. To our knowledge, the analyses herein represent the largest (and only second to date) series of utilizing connectivity based DTI segmentation of thalamus to evaluate DBS electrode positioning for chronic pain in relation to the VPL/VPM sensory nuclei. This involved registering preoperative imaging to

postoperative MRI or CT scan data after electrode placement, inherently introducing room for error as the displacement of brain structures after electrode implantation can offset anatomic detail. Although this effect is likely to be minimal, it may not be negligible. Additionally, although our results suggest a promising role for tractography based thalamic segmentation in enhancing thalamic neuromodulation, the retrospective nature of our study and our limited sample size preclude definitive conclusions. At minimum, our results enable appreciation of the interpatient variability in thalamic nuclear distribution and prompt further investigation of these methods, while also providing an explanation for the failures of DBS for chronic pain with functional radiographic correlation in regards to lead placement.

CONCLUSION

Not all subcortical targets utilized in DBS based therapies have well defined anatomic boundaries on the currently available imaging systems used for stereotactic planning. In addition, many off-label indications for DBS have shown moderate and inconsistent efficacy, possibly as a result of poor stereotactic localization on account of this inability to discern functional anatomy on current imaging. We have previously demonstrated that diffusion-based tractography can be used to delineate the functional nuclei of the thalamus. Using these methods, we were able to retrospectively show that this DTI based segmentation can help predict which patients will respond better to DBS for chronic pain. In the future, diffusion based segmentation of the thalamus and other subcortical structures may be of great importance in helping guide the stereotactic localization of DBS targets to maximize clinical efficacy.

Acknowledgments

Sources of Support: National Institute of Biomedical Imaging and Bioengineering, Award Number K23EB014326 (N.P.) UCLA Department of Neurosurgery Visionary Ball, National Institute of Health R25 Training Grant Award (W.K.)

We would like to thank Dr. Antonio De Salles whose patients comprised the majority of the cases in this study. We would also like to acknowledge Erik Behnke whose assistance with the neurophysiological testing and equipment within the operating room is indispensible.

Funding

This work is supported by funds provided by National Institute of Biomedical Imaging and Bioengineering under Award Number K23EB014326 (N.P.) and the UCLA Department of Neurosurgery Visionary Ball. In addition it is supported in part by the National Institute of Health R25 training grant (W.K.).

References

1. Gol A. Relief of pain by electrical stimulation of the septal area. J Neurol Sci. 1967; 5:115–120. [PubMed: 6061755]
2. Levy R, Deer TR, Henderson J. Intracranial neurostimulation for pain control: a review. Pain Physician. 2010; 13:157–165. [PubMed: 20309382]
3. Bittar RG, Kar-Purkayastha I, Owen SL, Bear RE, Green A, Wang S, Aziz TZ. Deep brain stimulation for pain relief: a meta-analysis. J Clin Neurosci. 2005; 12:515–519. [PubMed: 15993077]
4. Abosch A, Yacoub E, Ugurbil K, Harel N. An assessment of current brain targets for deep brain stimulation surgery with susceptibility-weighted imaging at 7 tesla. Neurosurgery. 2010; 67:1745–1756. [PubMed: 21107206]

5. Richardson RM, Ostrem JL, Starr PA. Surgical repositioning of misplaced subthalamic electrodes in Parkinson's disease: location of effective and ineffective leads. Stereotact Funct Neurosurg. 2009; 87:297–303. [PubMed: 19641340]
6. Coenen VA, Allert N, Madler B. A role of diffusion tensor imaging fiber tracking in deep brain stimulation surgery: DBS of the dentato-rubro-thalamic tract (drt) for the treatment of therapy-refractory tremor. Acta Neurochir. 2011; 153:1579–1585. [PubMed: 21553318]
7. Hyam JA, Owen SL, Kringelbach ML, Jenkinson N, Stein JF, Green AL, Aziz TZ. Contrasting connectivity of the ventralis intermedius and ventralis oralis posterior nuclei of the motor thalamus demonstrated by probabilistic tractography. Neurosurgery. 2012; 70:162–169. [PubMed: 22158304]
8. Klein JC, Barbe MT, Seifried C, Baudrexel S, Runge M, Maarouf M, Gasser T, Hattingen E, Liebig T, Deichmann R, Timmermann L, Weise L, Hilker R. The tremor network targeted by successful VIM deep brain stimulation in humans. Neurology. 2012; 78:787–795. [PubMed: 22377809]
9. Pouratian N, Zheng Z, Bari AA, Behnke E, Elias WJ, Desalles AA. Multi-institutional evaluation of deep brain stimulation targeting using probabilistic connectivity-based thalamic segmentation. J Neurosurg. 2011; 115:995–1004. [PubMed: 21854118]
10. Sudhyadhom A, McGregor K, Okun MS, Foote KD, Trinastic J, Crosson B, Bova FJ. Delineation of motor and somatosensory thalamic subregions utilizing probabilistic diffusion tractography and electrophysiology. J Magn Reson Imaging. 2013; 37:600–609. [PubMed: 23060259]
11. Tu Z, Narr KL, Dollar P, Dinov I, Thompson PM, Toga AW. Brain anatomical structure segmentation by hybrid discriminative/generative models. IEEE Trans Med Imaging. 2008; 27:495–508. [PubMed: 18390346]
12. Dinov I, Lozev K, Petrosyan P, Liu Z, Eggert P, Pierce J, Zamanyan A, Chakrapani S, Van Horn J, Parker DS, Magsipoc R, Leung K, Gutman B, Woods R, Toga A. Neuroimaging study designs, computational analyses and data provenance using the LONI pipeline. PLoS One. 2010; 5:e13070. [PubMed: 20927408]
13. Boccard SG, Pereira EA, Moir L, Aziz TZ, Green AL. Long-term outcomes of deep brain stimulation for neuropathic pain. Neurosurgery. 2013; 72:221–230. [PubMed: 23149975]
14. Coffey RJ. Deep brain stimulation for chronic pain: results of two multicenter trials and a structured review. Pain Med. 2001; 2:183–192. [PubMed: 15102250]
15. Hamani C, Schwalb JM, Rezai AR, Dostrovsky JO, Davis KD, Lozano AM. Deep brain stimulation for chronic neuropathic pain: long-term outcome and the incidence of insertinal effect. Pain. 2006; 125:188–196. [PubMed: 16797842]
16. Hosobuchi Y, Adams JE, Rutkin B. Chronic thalamic stimulation for the control of facial anesthesia dolorosa. Arch Neurol. 1973; 29:158–161. [PubMed: 4591720]
17. Katayama Y, Yamamoto T, Kobayashi K, Oshima H, Fukaya C. Deep brain and motor cortex stimulation for post-stroke movement disorders and post-stroke pain. Acta Neurochir Suppl. 2003; 87:121–123. [PubMed: 14518537]
18. Marchand S, Kupers RC, Bushnell MC, Duncan GH. Analgesic and placebo effects of thalamic stimulation. Pain. 2003; 105:481–488. [PubMed: 14527708]
19. Mazars G, Merienne L, Ciolocca C. Intermittent analgesic thalamic stimulation: Preliminary note. Rev Neurol. 1973; 128:273–279. [PubMed: 4774913]
20. Rasche D, Rinaldi PC, Young RF, Tronnier VM. Deep brain stimulation for the treatment of various chronic pain syndromes. Neurosurg Focus. 2006; 21:E8.
21. Spiegelmann R, Nissim O, Daniels D, Ocherashvilli A, Mardor Y. Stereotactic targeting of the ventrointermediate nucleus of the thalamus by direct visualization with high-field MRI. Stereotact Funct Neurosurg. 2006; 84:19–23. [PubMed: 16636642]
22. Vassal F, Coste J, Derost P, Mendes V, Gabrillargues J, Nuti C, Durif F, Lemaire JJ. Direct stereotactic targeting of the ventrointermediate nucleus of the thalamus based on anatomic 1. 5-T MRI mapping with a white matter attenuated inversion recovery (WAIR) sequence. Brain Stimul. 2012; 5:625–633. [PubMed: 22405744]
23. Kovanlikaya I, Heier L, Kaplitt M. Treatment of chronic pain: diffusion tensor imaging identification of the ventroposterolateral nucleus confirmed with successful deep brain stimulation. Stereotact Funct Neurosurg. 2014; 92:365–371. [PubMed: 25359091]

24. Behrens TE, Woolrich MW, Jenkinson M, Johansen-Berg H, Nunes RG, Clare S, Matthews PM, Brady JM, Smith SM. Characterization and propagation of uncertainty in diffusion-weighted MR imaging. Magn Reson Med. 2003; 50:1077–1088. [PubMed: 14587019]
25. Jones EG, Wise SP, Coulter JD. Differential thalamic relationships of sensory-motor and parietal cortical fields in monkeys. J Comp Neurol. 1979; 183:833–881. [PubMed: 105020]
26. Mercado R, Constantoyannis C, Mandat T, Kumar A, Schulzer M, Stoessl AJ. Expectation and the placebo effect in Parkinson's disease patients with subthalamic nucleus deep brain stimulation. Mov Disord. 2006; 21:1457–1461. [PubMed: 16721750]
27. Morel A, Magnin M, Jeanmonod D. Multiarchitectonic and stereotactic atlas of the human thalamus. J Comp Neurol. 1997; 387:588–630. [PubMed: 9373015]
28. Nandi D, Aziz TZ. Deep brain stimulation in the management of neuropathic pain and multiple sclerosis tremor. J Clin Neurophysiol. 2004; 21:31–39. [PubMed: 15097292]
29. Turnbull IM, Shulman R, Woodhurst WB. Thalamic stimulation for neuropathic pain. J Neurosurg. 1980; 52:486–493. [PubMed: 6966326]
30. Yamada K, Akazawa K, Yuen S, Goto M, Matsushima S, Takahata A, Nakagawa M, Mineura K, Nishimura T. MR imaging of ventral thalamic nuclei. AJNR Am J Neuroradiol. 2010; 31:732–735. [PubMed: 19926703]
31. Zhang D, Snyder AZ, Shimony JS, Fox MD, Riachle ME. Noninvasive functional and structural connectivity mapping of the human thalamocortical system. Cereb Cortex. 2010; 20:1187–1194. [PubMed: 19729393]
32. Hunsche S, Sauner D, Runge MJ, Lenartz D, El Majdoub F, Treuer H, Sturm V, Maarouf M. Tractography-guided stimulation of somatosensory fibers for thalamic pain relief. Stereotact Funct Neurosurg. 2013; 91:328–334. [PubMed: 23969597]
33. Zrinzo L, Foltynie T, Limousin P, Hariz MI. Reducing hemorrhagic complications in functional neurosurgery: a large case series and systematic literature review. J Neurosurg. 2012; 116:84–94. [PubMed: 21905798]

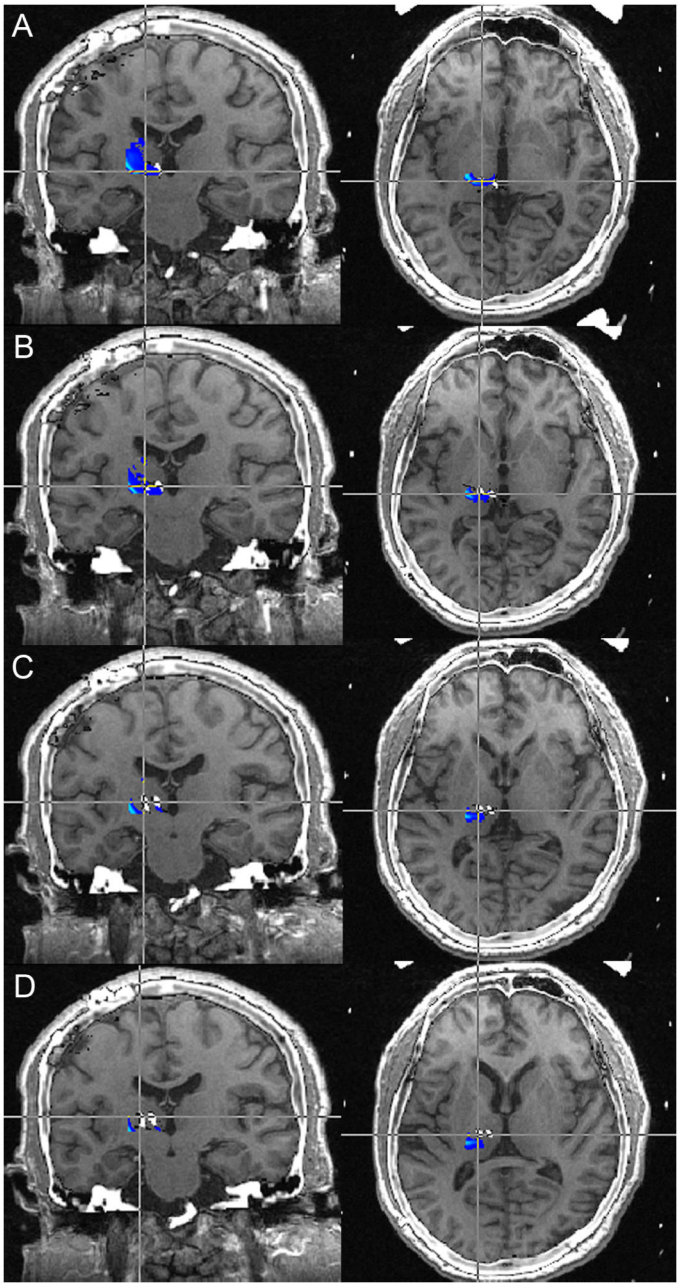

Figure 1.

Preoperative MRI-postoperative CT fusion for Patient 2. The DBS lead for all contacts 0–3 (A–D) are medial to the regions of the thalamus to have the highest probability of being VPL/VPM.

MRI: magnetic resonance imaging; CT: computed tomography; DBS: deep brain stimulation; VPL/VPM: ventroposterolateral/ventroposteromedial thalamus

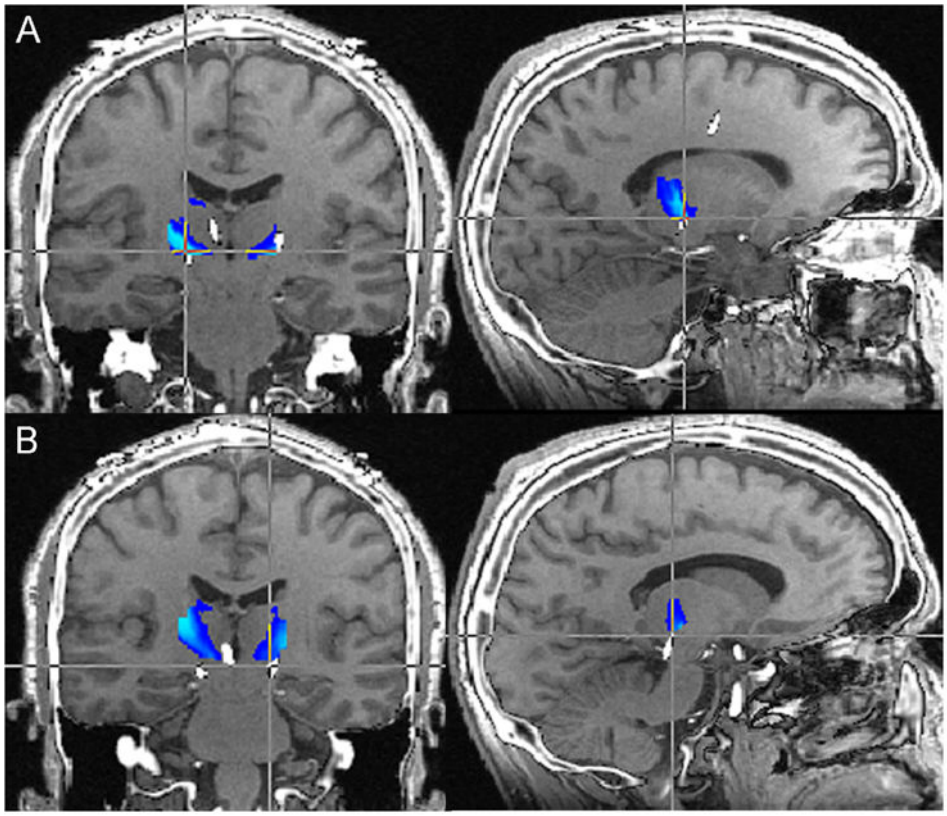

Figure 2.

Preoperative MRI-postoperative CT fusion for Patient 1. Contact 3 (right lead, Figure 1A) was the only contact dorsal enough to be within the sensory thalamus. The dorsal-most contact of the left lead (contact 7, Figure 1B) was below the level of the tractography determined sensory thalamus.

MRI: magnetic resonance imaging; CT: computed tomography

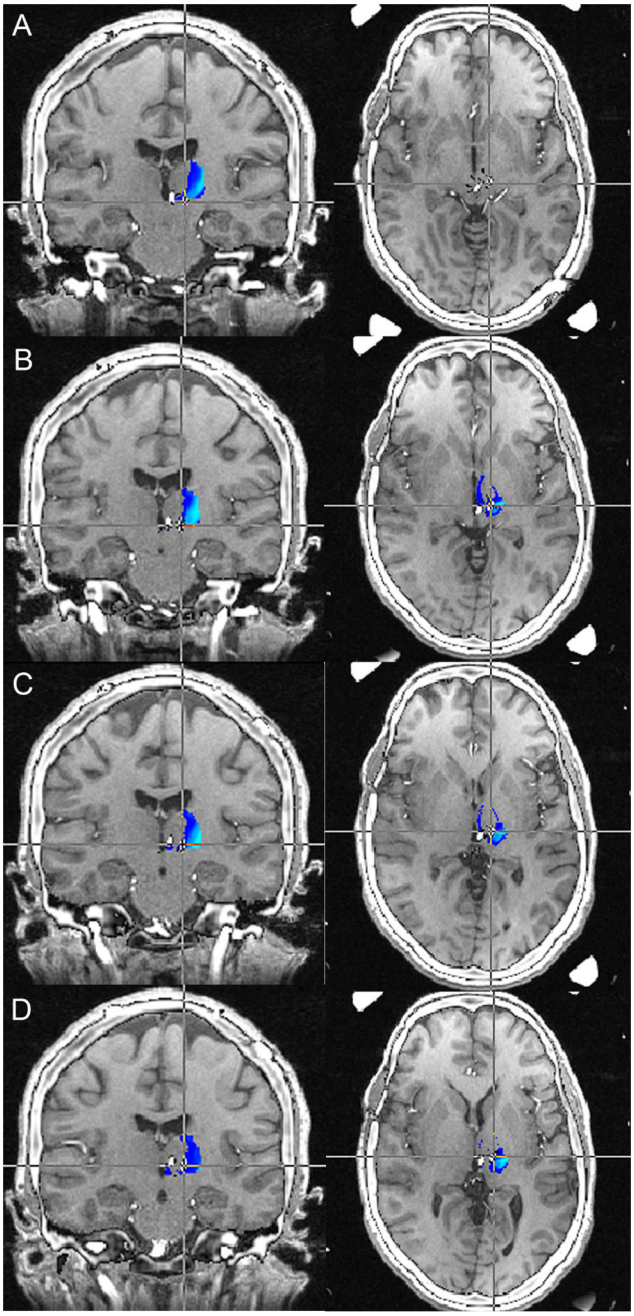

Figure 3.

Preoperative MRI-postoperative CT fusion for Patient 3. The probabilistic tractography determined sensory thalamus is shown in blue-light blue, with light blue indicating regions with the greatest probability of being sensory thalamus. Each set of images represents a specific lead position, with A=0, B=1, C=2, and D=3. The patient had the greatest clinical response to contacts 1 and 2 (B and C), with noted greatest overlap with the light blue regions with these lead positions.

MRI: magnetic resonance imaging; CT: computed tomography

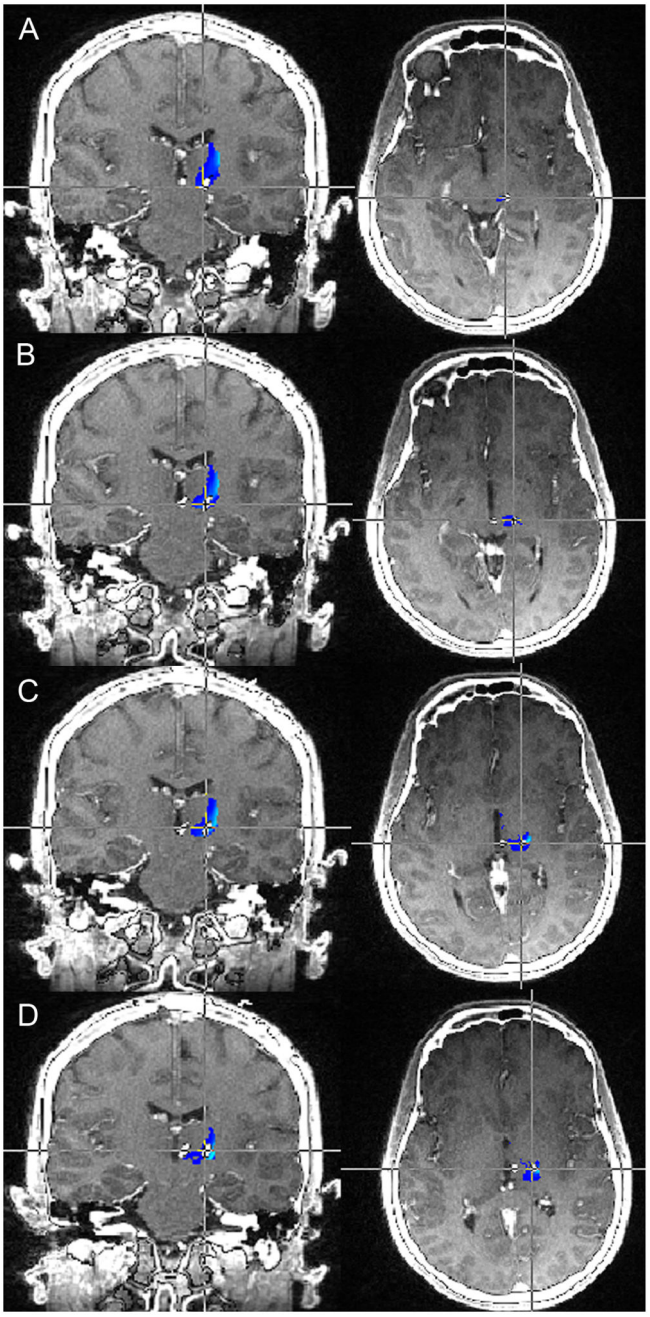

Figure 4.

Preoperative MRI-postoperative CT fusion for Patient 5. Image fusion demonstrates excellent placement of the DBS electrode within the VPL/VPM thalamus. Contacts 1, 2, and 3 (B, C, and D respectively) are situated the most accurately within the areas with the greatest probability of containing sensory thalamus fibers (light blue). Contact 0 (A) is just out the region of greatest likelihood of being sensory thalamus, however is still within the general vicinity.

MRI: magnetic resonance imaging; CT: computed tomography; DBS: deep brain stimulation; VPL/VPM: ventroposterolateral/ventroposteromedial thalamus

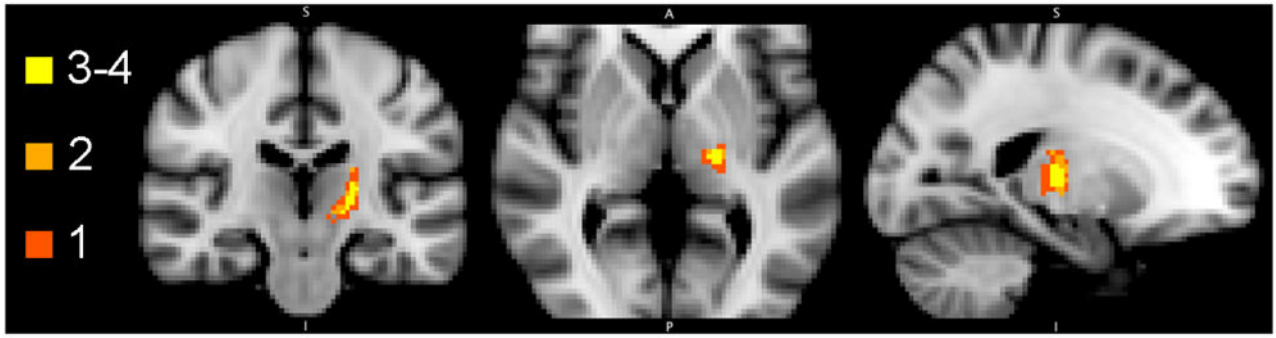

Figure 5.

Distribution of patient sensory thalamus representation by voxel. Four of the five patients had preoperative imaging that could be transferred into standard MNI space via a non-linear image registration transformation (FNIRT). Each color represents the number of patients whose sensory thalami overlap at a particular voxel. Light yellow represents voxels that contain sensory thalamus representation from 4 patients (4 voxels) as well as 3 patients (36 voxels). Light orange represents voxels that contain sensory thalamus representation from only 2 patients (38 voxels). Dark orange represents voxels that contain representation from only one patient (108 voxels).

Table 1

Presenting patient demographics

Patient	Gender	Age at DBS	Indication	Duration of symptoms	Prior surgery	DBS target
1	M	46 years	SCI and neuropathic pain	2 years	Lumbar fusion	B VPL & PAG
2	F	47 years	Brachial plexus avulsion	11 years	Stellate ganglionectomy; motor cortex stimulation	R VPM/VPL & PAG
3	F	48 years	Dejerine Roussy syndrome	2 years	L parietal epidural stimulator trial	L VPM/VPL & PAG
4	M	81 years	Postherpetic neuralgia	7 years	R ventralis caudalis deep brain stimulation	R VPM/VPL & PAG
5	F	58 years	Brachial plexus scarring, RSD	25 years	R anterior scalenectomy, sympathectomy, 1st rib resection; neurolysis; steroid injections; intrathecal pain pump placement; SCS	L VPL & PAG

DBS, deep brain stimulation; SCI, spinal cord injury; VPL, ventral posterolateral nucleus; PAG, periaqueductal gray; R, right; L, left; VPM, ventral posteromedial nucleus; PVG, periventricular gray; RSD, reflex sympathetic dystrophy; SCS, spinal cord stimulation

Table 2

Deep brain stimulation intraoperative macrostimulation and clinical follow up data

Patient	DBS Target	Intraoperative repositioning	Electrode position relative to DTI	Postoperative procedures	Follow up (months)	Outcome	Maximum pain reduction	Pain reduction at last follow up
1	B VPL & PVG	R once, 2mm laterally L twice, total 2mm laterally	Inferior, then within target	Thalamic leads retracted 6mm	48	Stabbing resolved, burning (40%)	6	6
2	R VPM/VPL & PVG	On target	Far medial	Spinal cord stimulation	35	No relief	4	1
3	L VPM/VPL & PVG	On target	Within target	None	2	Adequate pain control	7	7
4	R VPM/VPL & PVG	Once, 2mm medially	Too medial (outskirts of VPL/VPM)	RFA of L SPG	45	No benefit for 1 year, then thalamic stimulation discontinued and had relief for 1 year. Then failed and opted for RFA.	8	2
5	L VPL & PVG	Once, 2mm posteriorly	Within target	None	14	Persistent relief	3	3

DBS, deep brain stimulation; DTI, diffusion tensor imaging; B, bilateral; VPL, ventral posterolateral nucleus; PVG, periventricular gray; R, right; L, left; VPM, ventral posteromedial nucleus; RFA, radiofrequency ablation; SPG, sphenopalatine ganglion

Table 3

Final lead positioning

			Final distal lead coordinates relative to MCP			AC-PC (mm)
Patient	**Target**	**Intraoperative repositioning**	**x**	**y**	**Z**	
1	B VPL & PAG	R once, 2mm laterally L twice, total 2mm laterally	L VPL 10.67 R VPL 12.17	L VPL −16.35 R VPL −12.06	L VPL −13.45 R VPL −8.02	23.92
2	R VPM/VPL & PAG	On target	R VPL 12.86 R PVG 3.69	R VPL −8.94 R PVG −12.43	R VPL −0.64 R PVG −3.07	24.32
3	L VPM/VPL & PAG	On target	L VPL 11.62 L PVG 3.5	L VPL −9.92 L PVG −11.66	L VPL 0 L PVG 0	24.80
4	R VPM/VPL & PAG	Once, 2mm medially	R PVG 7.40 R VPM 11.54	R PVG −10.69 R VPM −9.91	R PVG −0.10 R VPM −1.90	28.31
5	L VPL & PAG	Once, 2mm posteriorly	L PVG 0.84 L VPL 11.97	L PVG −11.77 L VPL 13.73	L PVG −1.70 L VPL −3.56	27.33

MCP, mid-commissural point; AC-PC, anterior commissure to posterior commissure length; B, bilateral; VPL, ventral posterolateral; PAG, periaqueductal gray; R, right; L, left; VPM, ventral posteromedial

Note: Along the x-axis, positive coordinates indicate positioning to the right of the origin; along the y-axis, positive coordinates indicate anterior positioning relative to the origin; along the z-axis, positive coordinates indicate superior positioning relative to the origin